Non-equilibrium Majorana fluctuations

2017 New J. Phys. 19 063020

(http://iopscience.iop.org/1367-2630/19/6/063020)

New Journal of Physics
The open access journal at the forefront of physics

Deutsche Physikalische Gesellschaft DPG
IOP Institute of Physics

Published in partnership with: Deutsche Physikalische Gesellschaft and the Institute of Physics

OPEN ACCESS

RECEIVED
22 December 2016

REVISED
27 March 2017

ACCEPTED FOR PUBLICATION
3 May 2017

PUBLISHED
16 June 2017

PAPER

Non-equilibrium Majorana fluctuations

Sergey Smirnov

Institut für Theoretische Physik, Universität Regensburg, D-93040 Regensburg, Germany
P. N. Lebedev Physical Institute of the Russian Academy of Sciences, 119991 Moscow, Russia

E-mail: sergey.smirnov@physik.uni-regensburg.de **and** ssmirnov@sci.lebedev.ru

Keywords: Majorana fermions, non-equilibrium noise, effective charge

Abstract

Non-equilibrium physics of random events, or fluctuations, is a unique fingerprint of a given system. Here we demonstrate that in non-interacting systems with dynamics driven essentially by Majorana states the effective charge e^*, characterizing the electric current fluctuations, is fractional. This is in contrast to non-interacting Dirac systems with the trivial electronic charge $e^* = e$. In the Majorana state, however, we predict two different fractional effective charges at low and high energies, $e_{\rm l}^* = e/2$ and $e_{\rm h}^* = 3e/2$, accessible at low and high bias voltages, respectively. We show that while the low-energy effective charge $e_{\rm l}^*$ is sensitive to thermal fluctuations of the current, the high-energy effective charge $e_{\rm h}^*$ is robust against thermal noise. A unique fluctuation signature of Majorana fermions is therefore encoded in the high-voltage tails of the electric current noise easily accessible in experiments on strongly non-equilibrium systems even at high temperatures.

1. Introduction

The physics of fluctuation phenomena, or noise, dating back to Brownian [1] motion has received a systematic scientific framework since Einstein's [2] and Smoluchowski's [3] conceptual theoretical breakthroughs proven experimentally by Svedberg [4] and Perrin [5]. Spontaneous or externally excited fluctuations are an extremely insightful tool, known as fluctuation spectroscopy. Due to their sensitivity, fluctuations can scan the microscopic structure in much more detail than mean values.

In equilibrium, nevertheless, the kinetics of a given system makes a clever link between random deviations of its physical quantities from mean values and the mean values themselves. This link, dating back to the Nyquist's [6] and Callen's and Welton's [7] fundamental discoveries, is known as the fluctuation-dissipation theorem [8].

In non-equilibrium the fluctuation-dissipation theorem breaks down, and for a given system its fluctuation physics deviates from the mean value description. Here non-equilibrium noise might be comparable to or, in fact, become stronger than the equilibrium noise. It is therefore a reliable and comprehensive method for conclusively revealing the microscopic structure of a system when measurements of its mean quantities are physically inconclusive.

This is what currently happens in dealing with materialization of a particle cloning its own antiparticle. Namely, via unpairing Majorana [9] fermions, forming a single Dirac fermion, it is hoped that by implementation [10–13] of Kitaev's [14] model a single Majorana state will be detected [15–17]. Here experiments mainly focus on measurements [18] of mean quantities such as the differential conductance, which should exhibit a peak equal to one-half of the Dirac unitary limit [19]. This is inconclusive because such a peak might result, for example, from the Kondo effect [20] in an asymmetric mesoscopic system. This problem is inherent to Majorana's transport experiments dealing with mean values. Nevertheless, it is possible to get a conclusive signature of Majorana fermions from the mean value description of both Majorana transport [21–26] and Majorana thermodynamics [27].

The freedom to involve non-equilibrium noise [28–31] in the fluctuation spectroscopy of Majorana fermions takes transport experiments on Majorana physics to a new level and makes them more interesting. This is because, as mentioned above, fluctuations usually bring conclusive information on the microscopic structure

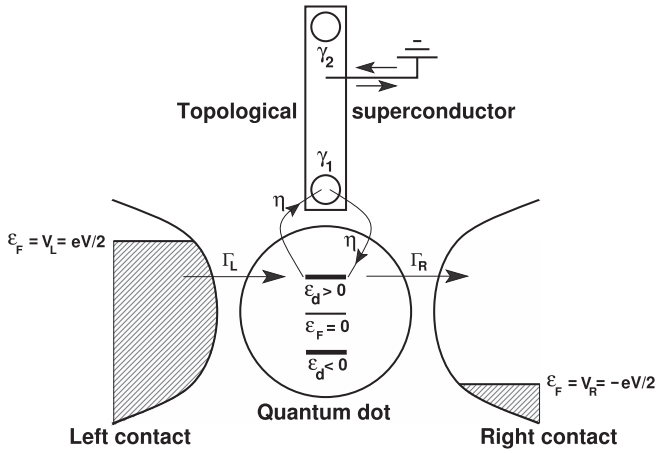

Figure 1. A quantum dot with a single-particle non-degenerate energy level ϵ_d is linked via tunneling mechanisms to two normal contacts and to one end of a one-dimensional topological superconductor supporting two Majorana bound states, γ_1, γ_2, at its ends. Here Γ_L and Γ_R characterize the tunneling strength between the left (L) and right (R) contacts while η is the strength of the tunneling between the quantum dot and the Majorana bound state γ_1. A bias voltage V may be applied to the contacts and induce an electric current flowing in the direction of arrows. The electric current $\langle I(t)\rangle$ and its noise $\langle I(t)I(t')\rangle$ may be measured in one of the contacts, for example in the left contact $\langle I_L(t)\rangle$, $\langle I_L(t)I_L(t')\rangle$.

of a system and at the same time these are transport experiments which are in general simpler than thermodynamic ones. So far Majorana noise has mainly been discussed with regard to linear responses. However, the real beauty of non-equilibrium noise is still to be explored beyond linear responses. Here fluctuations of the electric current may be characterized by the so-called effective charge e^* which is not directly related to a particle's elementary charge but rather characterizes backscattering processes [32]. Modern experiments [33] have already reached a remarkable accuracy and enable one to measure the noise of the electric current, making e^* a unique fluctuation fingerprint of the system.

In the present work we explore strongly non-equilibrium fluctuations of the electric current flowing through a non-interacting quantum dot coupled to a topological superconductor supporting at its ends two Majorana bound states implemented via the Kitaev chain model. It is well known that in the absence of Majorana fermions the effective charge for a non-interacting quantum dot is trivial and identical to the electronic charge, $e^* = e$. Here we demonstrate that in the presence of Majorana fermions (1) the effective charge fractionalizes to (2) $e_l^* = e/2$ at low energies and to (3) $e_h^* = 3e/2$ at high energies and show that (4) even when the low-energy effective charge $e_l^* = e/2$ is washed out by, for example, thermal noise, the high-energy effective charge $e_h^* = 3e/2$ is robust and persists up to very high temperatures providing a simple and reliable experimental platform for a unique signature of Majorana fermions out of strongly non-equilibrium fluctuations.

This paper is organized as follows. In section 2 we present a Majorana setup suitable for experiments on non-equilibrium noise and explore it using the Keldysh field integral framework. The results on non-equilibrium noise, in particular on the effective charge, are shown and discussed in section 3. We conclude with section 4. Appendices A and B provide details on the Keldysh field integral in the presence of Majorana fermions.

2. Theoretical setup and its Keldysh field integral description

Let us consider a setup similar to that of [27]. It represents a non-interacting quantum dot coupled via tunneling interaction to two (L and R) non-interacting contacts. In contrast to the equilibrium setup of [27], here the contacts may be used to apply a bias voltage V to the quantum dot, $V_L = -V_R = V/2$, $V_L - V_R = V$, as shown schematically in figure 1 for the case $V < 0$. The quantum dot has only one single-particle level which is spin non-degenerate, which may be experimentally implemented, for example, via Zeeman splitting which also filters out the Kondo effect [20, 34]. Note also that below we explore strongly non-equilibrium states which are accessed at very high bias voltage V so that the Kondo state is totally ruined [35] anyway and therefore does not lead to any experimental ambiguity. Finally, similar to [27], the quantum dot interacts via another tunneling mechanism with a grounded topological superconductor supporting at its ends two Majorana bound states.

To give the problem a concrete and mathematically convenient treatment we formulate it in terms of the quantum many-particle Keldysh Lagrangian $\mathcal{L}_\mathcal{K}(q, p) = \sum_i i\hbar q_i \dot{p}_i - \mathcal{H}_\mathcal{K}(q, p)$ which constitutes the basis for the Keldysh action $\mathcal{S}_\mathcal{K}$. Here the momenta p_i and coordinates q_i are the fermionic coherent states of the system and their conjugate partners, respectively. The Lagrangian formulation is fully equivalent to the quantum Hamiltonian $\mathcal{H}_\mathcal{K}(q, p)$ formulation but has a certain technical advantage in calculating strongly

non-equilibrium fluctuations of the electric current via the Keldysh field integral [36], which we employ below to obtain the current–current correlation function.

For the quantum dot ($p = \psi, q = \bar{\psi}$), contacts ($p = \phi, q = \bar{\phi}$) and tunneling between them we, respectively, have:

$$\mathcal{H}_{\rm QD}(q, p) = \epsilon_{\rm d}\bar{\psi}(t)\psi(t), \tag{1}$$

where $\epsilon_{\rm d}$ is the quantum dot energy level and the real time t runs along the Keldysh closed contour $\mathcal{C}_\mathcal{K}$, $t \in \mathcal{C}_\mathcal{K}$,

$$\mathcal{H}_{\rm C}(q, p) = \sum_{l=\{\rm L,R\};k_l} \epsilon_{lk_l}\bar{\phi}_{lk_l}(t)\phi_{lk_l}(t), \tag{2}$$

where below we will assume identical quantum numbers k_l in both L and R contacts as well as large contacts so that their spectrum ϵ_{lk_l} is continuous and their density of states $\nu_{\rm C}$ is constant in the vicinity of the Fermi energy,

$$\mathcal{H}_{\rm DT}(q, p) = \sum_{l=\{\rm L,R\};k_l} T_{lk_l}\bar{\phi}_{lk_l}(t)\psi(t) + \text{H.c.} \tag{3}$$

We use for the Dirac tunneling the standard assumption that the tunneling matrix elements weakly depend on the quantum numbers of the contacts, $T_{lk_l} \approx T_l$. This allows us to characterize the tunneling coupling by the energy scales $\Gamma_l = \pi\nu_{\rm C}|T_l|^2$ or $\Gamma \equiv \Gamma_{\rm L} + \Gamma_{\rm R}$.

Finally, the topological ($p = \zeta, q = \bar{\zeta}$) part of the Hamiltonian is given as the sum of the Hamiltonians of the topological superconductor and its tunneling interaction with the quantum dot:

$$\mathcal{H}_{\rm TS}(q, p) = {\rm i}\xi\bar{\zeta}_2(t)\zeta_1(t)/2, \tag{4}$$

where ξ is the energy originating from the overlap of the Majorana bound states ζ_1 and ζ_2 (in particular, $\xi = 0$ if there is no overlap as in sufficiently long Kitaev's chains),

$$\mathcal{H}_{\rm MT}(q, p) = \eta^*\bar{\psi}(t)\zeta_1(t) + \text{H.c.}, \tag{5}$$

where the Majorana tunneling entangles the Dirac fermions of the quantum dot with only one Majorana state, ζ_1, and is characterized by the energy scale $|\eta|$.

Due to the fundamental property of the Majorana fields, $\bar{\zeta}_j(t) = \zeta_j(t), j = 1, 2$, and the canonical fermionic anticommutation relations the field integral for the Keldysh partition function,

$$\mathcal{Z}_\mathcal{K} = \int \mathcal{D}(p, q)\exp\left(\frac{\rm i}{\hbar}\mathcal{S}_\mathcal{K}\right), \tag{6}$$

is a functional integral with the constraints $\bar{\zeta}_j(t) = \zeta_j(t)$, $\zeta_j^2(t) = 1$ which might be viewed as fermionic constraints imposed at any given discrete time of the Keldysh closed contour. Nevertheless, since $\mathcal{H}_\mathcal{K}$ is quadratic in all p_i, q_i, this field integral may be solved exactly as in many standard textbooks [36], as explained in detail in appendices A and B.

Using an imaginary time field theory, it has been rigorously proven [27] by entropic reasoning that a macroscopic state of the above setup is Majorana dominated at low temperatures. Therefore, it must exhibit various fractionalizations [17] of its observables. Here, in particular, we are interested in fractionalizations of the electric current fluctuations.

To this end we introduce suitable sources into the Keldysh partition function (6) turning it into the Keldysh generating functional:

$$\mathcal{J}_\mathcal{K} = \int \mathcal{D}(p, q)\exp\left(\frac{\rm i}{\hbar}\mathcal{S}_\mathcal{K} + \sum_{l=\{\rm L,R\}}\int_{\mathcal{C}_\mathcal{K}} {\rm d}t\, J_l(t)I_l(t)\right), \tag{7}$$

where $J_l(t)$ is the source field and $I_l(t)$ is the electric current field. The mean current and current–current correlator are then obtained by proper functional differentiations of equation (7) with respect to the source field. Here, calculating the current–current correlator, one should remember that due to the topological superconductor (or fermionic constraints) various anomalous expectation values do not vanish, i.e. in general $\langle\psi_1\psi_2\bar{\psi}_3\bar{\psi}_4\rangle$ also includes the term $\langle\psi_1\psi_2\rangle\langle\bar{\psi}_3\bar{\psi}_4\rangle$.

Below we are interested in the so-called greater current–current correlator $S^>(t, t') \equiv \langle\delta I_{\rm L}(t)\delta I_{\rm L}(t')\rangle$ (as opposed to the lesser one, $S^<(t, t') \equiv \langle\delta I_{\rm L}(t')\delta I_{\rm L}(t)\rangle$), where $\delta I_{\rm L}(t) \equiv I_{\rm L}(t) - I_{\rm L}(V)$ is the electric current fluctuation field and $I_{\rm L}(V) \equiv \langle I_{\rm L}(t)\rangle$ is the mean electric current. More precisely, we calculate the Fourier component $S^>(\omega, V)$ as a function of the bias voltage V at zero frequency, $S^>(V) \equiv S^>(\omega = 0, V)$.

The essential and experimentally relevant characteristic of the electric current fluctuations is the effective charge e^* which relates the nonlinear parts of $S^>(V)$ and $I(V) \equiv I_{\rm L}(V)$. In modern experiments [33] on non-equilibrium current fluctuations in quantum dots one measures the shot noise, $S^>(V)$, and the mean current, $I(V)$, subtracts the linear parts to get the corresponding nonlinear quantities $S^>_{\rm K}(V)$, $I_{\rm K}(V)$ and finally obtains the ratio $e^*/e = S^>_{\rm K}(V)/e|I_{\rm K}(V)|$ at small bias voltages. In particular, for non-interacting quantum dots one gets the trivial result, $e^* = e$.

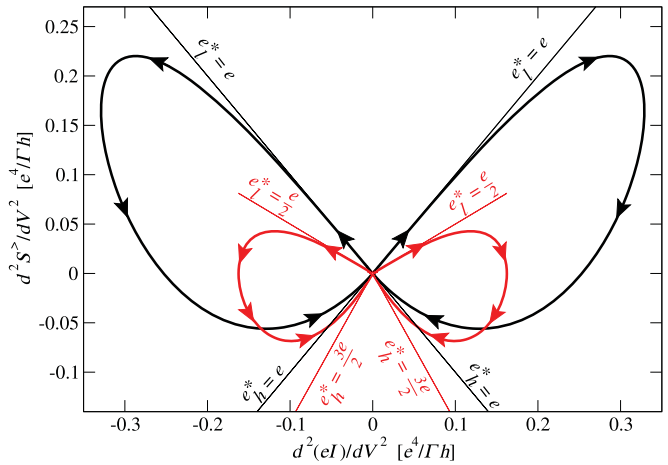

Figure 2. The second derivative of the current noise, $d^2S^>(V)/dV^2$, as a function of the second derivative of the mean current times the electronic charge e, $d^2[eI(V)]/dV^2$. The curves are parameterized by the bias voltage V which grows in the direction of the arrows from $e|V|/\Gamma = 10^{-3}$ to $e|V|/\Gamma = 10$. For both curves the temperature is the same, $k_BT/\Gamma = 10^{-6}$. The black curve is for $\xi/\Gamma = 10^2$. The red curve is for $\xi/\Gamma = 10^{-4}$.

We generalize the above definition of the effective charge in such a way that it not only reproduces the standard definition at small bias voltages but also provides a unique fluctuation fingerprint of a system far from equilibrium where the system's dynamics is highly nonlinear and the expansion in powers of V makes no sense at all. To this end we note that at small values of $|V|$ the nonlinear parts of both the shot noise and the mean current are cubic in V. Therefore, at low voltages the second derivatives $d^2S^>(V)/dV^2$ and $d^2I(V)/dV^2$ are linear in V and thus linearly depend on each other with the ratio $[d^2S^>(V)/dV^2]/|d^2[eI(V)]/dV^2| = S_K^>(V)/e|I_K(V)|$. Therefore, we define the effective charge as

$$\frac{e^*}{e} = \frac{\frac{d^2S^>(V)}{dV^2}}{\left|\frac{d^2[eI(V)]}{dV^2}\right|}, \tag{8}$$

which is applicable when the second derivatives linearly depend on each other. Note, that the linear dependence of $d^2S^>(V)/dV^2$ on $d^2I(V)/dV^2$ does not necessarily imply a linear dependence of these derivatives on the bias voltage. In fact, at large bias voltages expansions in powers of V do not exist while $d^2S^>(V)/dV^2$ may still linearly depend on $d^2I(V)/dV^2$ and, therefore, the effective charge in equation (8) makes sense even at extremely high bias voltages.

Note also that the definition in equation (8) is highly consistent because, as shown below, in the absence of Majorana fermions it gives for the non-interacting case $e^* = e$ at both low and very large bias voltages. Importantly, this definition is also highly relevant for experiments because each of the second derivatives may already be measured with sufficient accuracy at present.

3. Results and discussion

Let us consider the situation when $|\eta| > \Gamma$. We also currently assume $\epsilon_d = 0$ and $\Gamma_L = \Gamma_R$. Figure 2 shows $d^2S^>(V)/dV^2$ as a function of $d^2I(V)/dV^2$ when $|\eta| = 8\Gamma$ for two different values of the overlap energy ξ. The black curve is for $\xi/\Gamma = 10^2$. In this case the Majorana fermions strongly overlap, forming a single Dirac fermion leading to the current fluctuations with a trivial effective charge equal to the electronic charge at both low ($e|V| \ll \Gamma$) and high ($e|V| > \Gamma$) energies. Indeed, the curve is linear near the origin at both its starting point and its ending point with the tangent lines having unit absolute slope resulting in $e_l^* = e_h^* = e$. However, when $\xi/\Gamma = 10^{-4}$, Majorana bound states overlap weakly and the fluctuation physics is governed by fractional degrees of freedom leading to fractional effective charges at low and high energies. In this case the curve is linear near the origin at both its starting point and its ending point with the tangent lines having, respectively, absolute slopes equal to $1/2$ and $3/2$ resulting in $e_l^* = e/2$ at low energies ($e|V| \ll \Gamma$) and $e_h^* = 3e/2$ at high energies ($|\eta| > e|V| > \Gamma$). At voltages $e|V| \gg |\eta|$ the Majorana state is ineffective and the curve acquires a trivial linear character with $e^* = e$ which is not visible in figure 2 because both of the second derivatives become very small at the high-voltage tails of $S^>(V)$ and $I(V)$ shown in figure 3 for the case $\xi/\Gamma = 10^{-4}$. However, it becomes visible when the effective charge is plotted as a function of V (see figure 5 below).

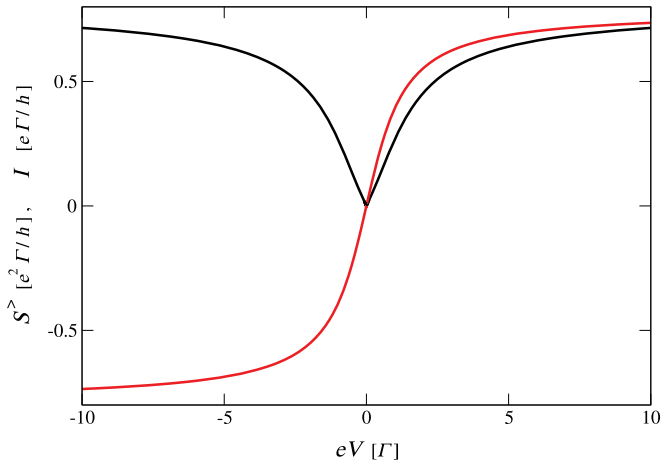

Figure 3. The current noise $S^>(V)$ (black, symmetric) and the mean current $I(V)$ (red, antisymmetric) as functions of the bias voltage V. For both curves $k_BT/\Gamma = 10^{-6}$ and $\xi/\Gamma = 10^{-4}$. For very small voltages $k_BT \ll e|V| \ll \Gamma$ both curves are almost linear with the slopes $dS^>(V)/dV = 0.25$, $dI(V)/dV = 0.5$ in full accordance with [28, 29] (Note that here we calculate the greater noise and not the symmetrized noise as in [28, 29]. For zero frequency they differ by a factor of 2.)

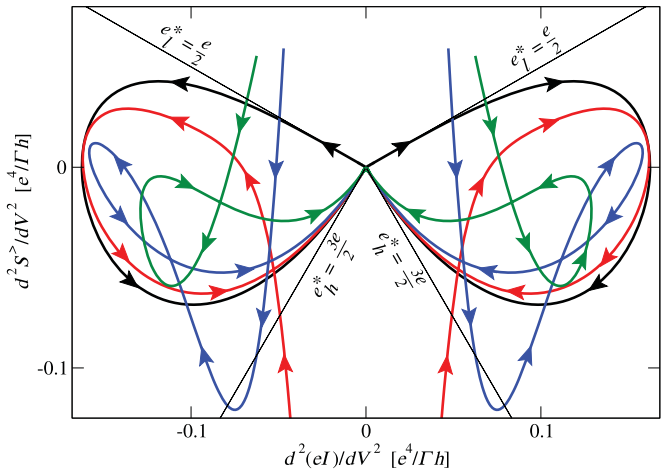

Figure 4. The second derivative of the current noise, $d^2S^>(V)/dV^2$, as a function of the second derivative of the mean current times the electronic charge e, $d^2[eI(V)]/dV^2$. For all the curves $\xi/\Gamma = 10^{-4}$. The temperatures are $k_BT/\Gamma = 10^{-6}$ (black), $k_BT/\Gamma = 10^{-2}$ (red), $k_BT/\Gamma = 3 \cdot 10^{-2}$ (blue) and $k_BT/\Gamma = 10^{-1}$ (green). The curves are parameterized by the bias voltage V which grows in the direction of the arrows from $e|V|/\Gamma = 10^{-3}$ to $e|V|/\Gamma = 10$ (black), from $e|V|/\Gamma = 8.85 \cdot 10^{-2}$ to $e|V|/\Gamma = 10$ (red), from $e|V|/\Gamma = 1.025 \cdot 10^{-1}$ to $e|V|/\Gamma = 10$ (blue) and from $e|V|/\Gamma = 2.15 \cdot 10^{-1}$ to $e|V|/\Gamma = 10$ (green). All the high-temperature curves start from positive values of $d^2S^>(V)/dV^2$. For the red curve the starting point is chosen so as not to overload the figure with its low-voltage or thermal noise branch going from large positive to large negative values of $d^2S^>(V)/dV^2$ since in the present research we do not focus on the thermal Majorana noise.

In figure 4 we show $d^2S^>(V)/dV^2$ as a function of $d^2I(V)/dV^2$ for $|\eta| = 8\Gamma$, $\xi/\Gamma = 10^{-4}$ for different temperatures. Since the overlap energy is small, the current fluctuations are essentially governed by the Majorana degrees of freedom. Here we increase the bias voltage of the starting points of the high-temperature curves to stay in the regime $e|V| > k_BT$ in order to avoid high values of the thermal Majorana noise which is not a focus of the present research. At high temperatures (red, blue and green curves) the low-energy effective charge $e_l^* = e/2$ is completely washed out by thermal fluctuations of the electric current. However, the high-energy effective charge $e_h^* = 3e/2$ is robust against thermal noise and persists up to very high temperatures, $k_BT/\Gamma = 10^{-1}$ (green curve).

Let us estimate the temperature at which the fractional high-energy effective charge $e_h^* = 3e/2$ might be observed in experiments. If the induced superconducting gap is taken from [19], $\Delta = 250\ \mu$eV, and $|\eta| \approx \Delta$, then we obtain $T \approx 36$ mK which is easily reachable in modern experiments. If the induced superconducting gap is taken from [37], $\Delta = 15$ meV, then $T \approx 2$ K which is even more reachable.

The fractional high-energy effective charge $e_h^* = 3e/2$ is perfectly achieved only at $|\eta| > e|V| \gg \Gamma$ which requires $|\eta| \gg \Gamma$. However, according to our numerical analysis we estimate that for $|\eta| > \Gamma$ (and small ξ) it

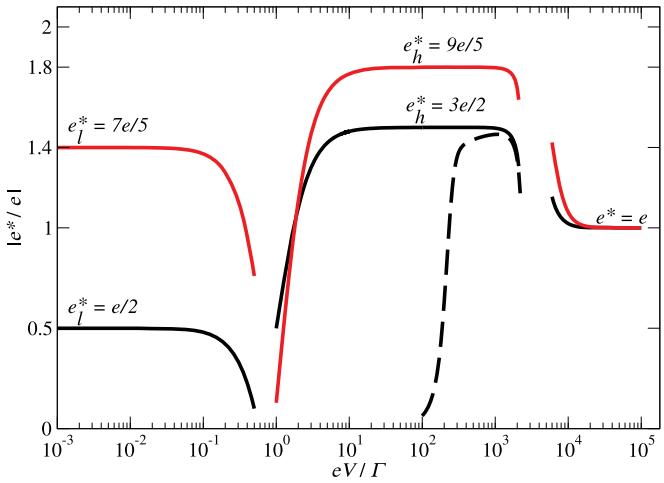

Figure 5. Effective charge as a function of the bias voltage. The black solid line corresponds to the case $\gamma_L = \gamma_R = 0.5$ while the red solid line corresponds to the case $\gamma_L = 0.8$, $\gamma_R = 0.2$. For both solid curves $k_B T/\Gamma = 10^{-6}$. The black dashed line corresponds to the case $\gamma_L = \gamma_R = 0.5$, $k_B T/\Gamma = 10^{-2}|\eta| = 10\,\Gamma$. In all cases the Majorana bound states overlap weakly, $\xi/\Gamma = 10^{-4}$, i.e. they are well defined and govern the non-equilibrium physics up to very high voltages $e|V| \sim |\eta|$. For extremely high voltages, $e|V| \gg |\eta|$, the Majorana state is ineffective. As a result, at $e|V| \gg |\eta|$ the effective charge becomes equal to the trivial electronic charge, $e^* = e$.

weakly deviates from the value $3e/2$. Namely, from numerical fitting we get $e_h^* \approx [3/2 - 2(\Gamma/\eta)^2]e$. So that $|\eta| = 8\Gamma$ gives $e_h^* \approx 1.47e$, $|\eta| = 20\Gamma$ gives $e_h^* \approx 1.495e$ and $|\eta| = 50\Gamma$ gives $e_h^* \approx 1.4992e$.

Importantly, by means of a gate voltage one may easily in realistic experiments increase ϵ_d so that $\epsilon_d > 0$, $|\epsilon_d| > \Gamma$. In this case the quantum dot is in the empty orbital regime [20] opposite to the Kondo one. In this way one fully eliminates [38] the Kondo effect. At the same time e_l^* and e_h^* do not change as soon as the quantum dot is in the Majorana universal regime, $|\eta| > \max\{|\epsilon_d|, \Gamma, e|V|\}$. Since Γ and/or $|\eta|$ may be easily varied in modern experiments [39], the Majorana universal regime is readily reachable in modern laboratories. Therefore, one may unambiguously observe in realistic experiments the universal plateaus $e_l^* = e/2$ and $e_h^* = 3e/2$ in the empty orbital and Majorana universal regime as it is shown in figure 5 for the case $|\eta|/\Gamma = 10^3$ and $\epsilon_d/\Gamma = 8$. These plateaus are universal and do not depend on ϵ_d as soon as $|\epsilon_d| < |\eta|$. Also for $|\eta|/\Gamma = 10^2$ the plot on figure 5 is almost unchanged. Moreover, we find that the e_h^* plateau survives up to very high temperatures, $k_B T \sim 10^{-2}|\eta|$, i.e. up to $k_B T = 10\,\Gamma$ for the present case as shown by the black dashed line in figure 5. As one can see, although the plateau e_h^* becomes very narrow at such a high temperature, it is still visible and it almost reaches the value $3e/2$ even at $k_B T = 10\,\Gamma$.

Another important aspect is the universality of the effective charge plateaus e_l^* and e_h^* when the quantum dot is asymmetrically coupled to the left and right contacts. This asymmetry may be characterized by the quantities $\gamma_L \equiv \Gamma_L/\Gamma$, $\gamma_R \equiv \Gamma_R/\Gamma$, which satisfy $\gamma_L + \gamma_R = 1$. The symmetric setup discussed above corresponds to the case $\gamma_L = \gamma_R = 0.5$. In a general setup $\gamma_L \neq \gamma_R$. Nevertheless, the effective charge e^* in equation (8) is characterized by two different universal plateaus e_l^* and e_h^* at low and high bias voltages, respectively. In this general asymmetric situation when $\gamma_L \neq \gamma_R$ and when ξ is small, i.e. the two Majorana bound states are well separated, the low-energy and high-energy plateaus of the effective charge are, respectively,

$$e_l^* = (3\gamma_L - 1)e, \quad e_h^* = (1 + \gamma_L)e. \tag{9}$$

We obtain these values with any desired numerical precision which means that equation (9) is the numerically exact result. Its analytical proof is a complicated task especially in the case of e_h^* taking place at high voltages where the dynamics is nonlinear. This analytical proof could be based on a semiclassical picture [40] and will be a challenge for our future research which should, in particular, explain the physical meaning of the high-energy effective charge e_h^* predicted currently by different numerical techniques with very high precision.

From equation (9) one can see that $e_h^* - e_l^* = 2(1 - \gamma_L)$. Only when $\gamma_L \to 1$ does one get a unique effective charge at both low and high energies, $e_l^* = e_h^* = 2e$. However, as soon as $0 \leqslant \gamma_L < 1$, the unique value, $2e$, of the effective charge splits into two different values. In the symmetric case, $\gamma_L = \gamma_R = 0.5$, one gets from equation (9) the result discussed above, $e_l^* = e/2$, $e_h^* = 3e/2$. However, when, for example, $\gamma_L = 0.8$, $\gamma_R = 0.2$, one gets from equation (9) $e_l^* = 7e/5$, $e_h^* = 9e/5$, as shown in figure 5. Once again, we emphasize that the low-energy, e_l^*, and high-energy, e_h^*, effective charge plateaus, given by equation (9), are universal for all possible values of the asymmetries γ_L, γ_R. In particular they do not depend on ϵ_d, i.e. they do not depend on the gate voltage.

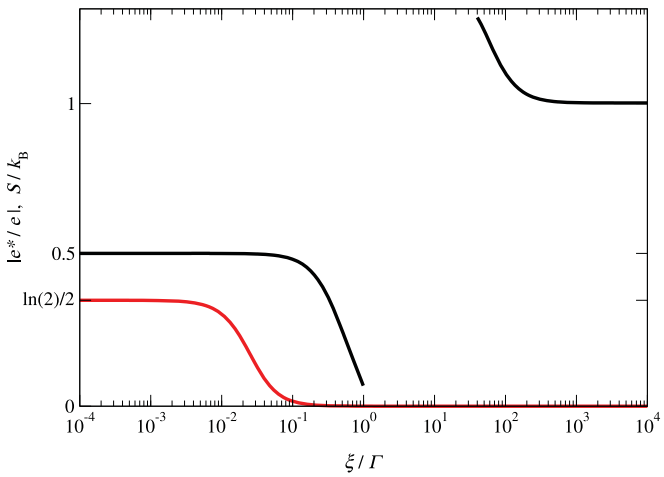

Figure 6. The effective charge $|e^*/e|$ (black line) as a function of the overlap energy ξ for $\epsilon_d/\Gamma = 8$, $k_B T/\Gamma = 10^{-8}$, $|\eta|/\Gamma = 10^3$, $e|V|/\Gamma = 10^{-2}$. The red line is the system's entropy S/k_B as a function of the overlap energy ξ for the same parameters but with zero bias voltage, $V = 0$. When the entropy is equal to the half-fermionic value, $S/k_B = \ln(2)/2$, the Majorana modes are well separated and they govern the equilibrium macroscopic state of the system. Weak deviations from this Majorana equilibrium macroscopic state occur at small bias voltages $k_B T \ll e|V| \ll \Gamma$. At these bias voltages the low-energy effective charge is equal to one-half of the electronic charge, $e_l^* = e/2$. At very large values of ξ the two Majorana modes strongly overlap and form one Dirac fermion. As a result, the entropy drops to the zero value corresponding to one non-degenerate ground state, namely the state with the quantum dot having zero electrons ($\epsilon_d > 0$). Weak deviations from this trivial equilibrium macroscopic state are characterized by the trivial value of the effective charge, $e^* = e$, when the bias voltage is small, $k_B T \ll e|V| \ll \Gamma$.

On the other hand, when ξ is large, i.e. when the two Majorana bound states strongly overlap to form a single Dirac fermion, we obtain with any desired numerical precision that $e_l^* = e_h^* = e$ for all γ_L, γ_R except for in the near vicinity of the point $\gamma_L = 1$, $\gamma_R = 0$, where e_l^* and e_h^* are sharply peaked to the value $e_l^* = e_h^* = 2e$ reached exactly at the point $\gamma_L = 1$, $\gamma_R = 0$. Therefore, in the case of large ξ, when the Majorana fermions form a single Dirac fermion, the effective charge plateaus, given by equation (9), do not appear for any degree of asymmetry described by the values of γ_L and γ_R.

This shows that the presence of two different universal effective charges at low and high energies, e_l^* and e_h^*, respectively, whose values are given by equation (9), is a unique fluctuation signature of the presence of Majorana fermions in a topological superconductor independent of the asymmetry in the coupling of the quantum dot to the left and right contacts. The experimental detection of at least one of these effective charges is enough to conclusively claim that the topological superconductor in this setup supports Majorana fermions.

Note also one practical aspect of equation (9). As soon as one of the effective charges, e_l^* or e_h^*, is detected in an experiment, the asymmetries γ_L and γ_R immediately follow in a simple way from equation (9). This simple way of extraction of γ_L and γ_R is definitely a practical advantage since usually in experiments it is difficult to measure the values of γ_L and γ_R. At the same time it is often necessary to know the values of γ_L and γ_R to theoretically describe realistic experiments.

We would like to emphasize that the low-energy effective charge e_l^* is obtained from equation (8) at $k_B T \ll e|V| \ll \Gamma$. Although the voltage is small here, $e|V| \ll \Gamma$, it is still finite to make thermal noise insignificant, $e|V| \gg k_B T$. Therefore the system is not in equilibrium. To understand how far it is from the equilibrium and to what extent its equilibrium macroscopic states may still govern the behavior of e_l^* we compare the behavior of e_l^* at $k_B T \ll e|V| \ll \Gamma$ with the behavior of the system's entropy at $V = 0$. Here it has been rigorously proven [27] that the macroscopic state of the present setup is characterized by the entropy plateau $S = \ln(2)/2$. This shows that the macroscopic state consists of a non-integer number of microscopic states, namely it consists of one-half of the Dirac fermion state. That the Majorana equilibrium macroscopic state indeed governs the behavior of e_l^* is clear from the following fact. When ξ grows, the two Majorana fermions combine into a single Dirac fermion and equation (8) gives a transition from the plateau $e_l^* = e/2$ to the plateau with the integer electronic charge $e^* = e$. At the same time, when ξ grows, the Majorana plateau $S = \ln(2)/2$ evolves into the trivial plateau $S = 0$ as shown in figure 6.

Concerning the high-energy effective charge we would like to note that its presence is also a unique signature of the Majorana fermions for all $0 < \gamma_L < 1$. This is particularly clear in the case $\gamma_L = \gamma_R = 0.5$. Here the noise properties characterized by $e_h^* = 3e/2$ cannot be induced by two-particle processes as one would expect from the standard point of view where an effective charge is usually associated with backscattering processes at $V \to 0$. From this traditional perspective one would conclude that $e_h^* = 3e/2$ is the result of a combination of single-particle and two-particle processes due to Andreev reflection. However, this traditional approach is

usually applied at $V \to 0$ [32, 33] and its adequacy at large bias voltages, where the dynamics is highly nonlinear, would be a question for future research, especially in connection with the definition of the effective charge given by equation (8). In the present case, however, this traditional point of view is definitely not applicable because for $\gamma_L = \gamma_R = 0.5$ the Andreev current, the only possible source of two-particle processes here, is equal to zero [29]. This shows that the traditional explanation of the high-energy effective charge in terms of combination of different processes is meaningless and the value $e_h^* = 3e/2$ is of pure Majorana nature. Likewise, when $\gamma_L \neq \gamma_R$, the effective charge e_h^* also has a Majorana nature although the Andreev current may be finite in this situation. Indeed, when $\gamma_L \neq \gamma_R$ the Majorana nature of the high-energy effective charge is obvious from the fact that it is fractional for small values of ξ when the Majorana modes are well separated but takes the trivial value $e^* = e$ as soon as the two Majorana fermions combine into a single Dirac fermion at large values of ξ, as has been discussed above.

Once more we would like to note that in the present research the term 'effective charge' in this high-voltage nonlinear regime is used just by analogy with the low-voltage regime and the precise meaning is given by the ratio in equation (8). However, as mentioned above, this ratio is experimentally relevant and can be measured with high precision at any voltage.

4. Conclusion

In conclusion, we have explored strongly non-equilibrium Majorana fluctuations of the electric current. It has been shown that in general these fluctuations are characterized by two fractional effective charges e_l^* and e_h^* at low and high energies, respectively. We have demonstrated that the low-energy effective charge e_l^* might be washed out by thermal noise but the high-energy effective charge e_h^* is robust and persists up to very high temperatures. The latter thus represents a challenge for modern experiments on noise phenomena in quantum dots since it is protected by high bias voltage V from all the perturbations with strength smaller than $e|V|$. In particular, electron–electron interactions and disorder will not change the high-energy effective charge if their characteristic energy scales, V_{e-e}, V_{dis}, are smaller than $e|V|$, that is if $V_{e-e} < e|V|$ and $V_{dis} < e|V|$. Of course in future our research should be improved with more realistic models to test the robustness of the high-energy effective charge and to predict its value when, for example, the density of states in the contacts is not constant or multiple levels in the quantum dot are involved in the transport. However, the model we have explored in the present research is already quite standard and is often applied in many other contexts to successfully describe modern experiments. We therefore believe that our results, in particular the high-energy effective charge, may become a reliable platform for a unique signature of Majorana fermions out of strongly non-equilibrium fluctuations.

Acknowledgments

We thank M Grifoni and W Izumida for important discussions. Support from the DFG under the program SFB 689 is acknowledged.

Appendix A. Majorana field operators in the Keldysh partition function

The partition function on the Keldysh closed time contour is usually [36] constructed by splitting this contour into small time intervals by writing the evolution operator as the product of elementary evolutions between neighboring discrete times. One then inserts the coherent state representation of the identity operator between all those elementary evolution operators and calculates the matrix elements of the elementary evolution operators between the fermionic coherent states $|\chi_{i-1}\rangle$ and $|\chi_i\rangle$ at neighboring discrete times $(i-1)$ and i. The corresponding matrix elements of fermionic creation and annihilation operators, $a_\alpha^\dagger$ and a_α (α is a single-particle index), may be written as [36]:

$$\langle \chi_i | a_\alpha^\dagger | \chi_{i-1} \rangle = \bar{\chi}_{i,\alpha} \langle \chi_i | \chi_{i-1} \rangle, \quad \langle \chi_i | a_\alpha | \chi_{i-1} \rangle = \frac{\partial \langle \chi_i | \chi_{i-1} \rangle}{\partial \bar{\chi}_{i,\alpha}}, \tag{A.1}$$

where $\chi_{i,\alpha}$ are the generators of the Grassmann algebra at discrete time i.

Therefore, the Majorana operator fields $\zeta_{1,2}$ obtained using equation (A.1) for the linear combinations of the Dirac fermion operators, $(f^\dagger + f)$ and $\mathrm{i}(f - f^\dagger)$, respectively, have the following form at a given discrete time i of the Keldysh closed time contour:

$$\zeta_{1,i} = \bar{\chi}_i + \frac{\partial}{\partial \bar{\chi}_i}, \quad \zeta_{2,i} = \mathrm{i}\left(\frac{\partial}{\partial \bar{\chi}_i} - \bar{\chi}_i\right). \tag{A.2}$$

Since the generators of the Grassmann algebra at a given discrete time i satisfy the anticommutation relation

$$\left[\bar{\chi}_i, \frac{\partial}{\partial \bar{\chi}_i}\right]_+ = 1, \tag{A.3}$$

the Majorana operator fields square to one at any given discrete time i of the Keldysh closed time contour,

$$\zeta_{1,i}^2 = \zeta_{2,i}^2 = 1. \tag{A.4}$$

In terms of the Dirac operator fields $\bar{\chi}, \chi$, the Hamiltonian $\mathcal{H}_{\mathrm{TS}}(q, p)$ from the main text takes the form at a given discrete time i:

$$\mathcal{H}_{\mathrm{TS}}(q, p) = \xi\left(\bar{\chi}_i \frac{\partial}{\partial \bar{\chi}_i} - \frac{1}{2}\right). \tag{A.5}$$

The constant term in equation (A.5) cancels out on the forward, '+', and backward, '−', branches of the Keldysh closed time contour and, therefore, plays no role.

Appendix B. Keldysh action

Since the overlap of any two fermionic coherent states, $|\psi\rangle$ and $|\phi\rangle$ has the form [36]:

$$\langle\psi|\phi\rangle = \exp\left(\sum_\alpha \bar{\psi}_\alpha \phi_\alpha\right), \tag{B.1}$$

one can see from equation (A.1) that in the calculation of the matrix elements of the elementary evolution operators the derivatives in equation (A.2) bring the generators χ_{i-1} at the discrete times neighboring the discrete times i, i.e. from the Grassmann algebras at the discrete times $(i - 1)$.

Therefore, in the calculation of the matrix elements the Majorana operator fields, $\zeta_{1,i}$ and $\zeta_{2,i}$, bring, respectively, in the continuum limit the factors $(\bar{\chi}(t) + \chi(t))$ and $\mathrm{i}(\chi(t) - \bar{\chi}(t))$, $t \in \mathcal{C}_\mathcal{K}$, while the Hamiltonian in equation (A.5) brings the factor $\xi\bar{\chi}(t)\chi(t)$, where the constant term in equation (A.5) is dropped, as explained above.

As a result, the Keldysh action $\mathcal{S}_\mathcal{K}$ from the main text may be written as

$$\mathcal{S}_\mathcal{K} = \mathcal{S}_0 + \mathcal{S}_\mathrm{T}, \tag{B.2}$$

where $\mathcal{S}_0$ is the conventional non-interacting (quadratic) action of the isolated quantum dot, contacts and topological superconductor and $\mathcal{S}_\mathrm{T}$ is the action which describes the tunneling interaction between the quantum dot and contacts as well as between the quantum dot and topological superconductor. It has the following form:

$$\begin{aligned}\mathcal{S}_\mathrm{T} = &-\int_{\mathcal{C}_\mathcal{K}} \mathrm{d}t\, \{\eta^*[\bar{\psi}(t)\chi(t) + \bar{\psi}(t)\bar{\chi}(t)] + \mathrm{H.c.}\} \\ &-\int_{\mathcal{C}_\mathcal{K}} \mathrm{d}t \sum_{l=\{L,R\};k_l} [T_l \bar{\phi}_{lk_l}(t)\psi(t) + \mathrm{H.c.}],\end{aligned} \tag{B.3}$$

where the notations are taken from the main text.

As one can see from equation (B.3), the only difference from the case of a field integral without the Majorana operator fields, equations (A.2)–(A.4), is the presence of anomalous terms in equation (B.3) such as $\bar{\psi}(t)\bar{\chi}(t)$. One deals with these terms in the same way as in the field integral theory of superconductivity [36] where the particle–hole space is introduced via the Nambu spinors. The additional particle–hole index, however, is technically inessential because the whole action is still quadratic and, therefore, is exactly solvable.

References

[1] Brown R 1828 *New Phil. J., Edinburgh* **5** 358
[2] Einstein A 1905 *Ann. Phys., Paris* **17** 549
[3] Smoluchowski M 1906 *Ann. Phys., Paris* **21** 772
[4] Svedberg T 1906 *Z. Elektrochem* **12** 853
[5] Perrin J 1908 *C.R. Acad. Sci., Paris* **146** 967
[6] Nyquist H 1928 *Phys. Rev.* **32** 110
[7] Callen H B and Welton T A 1951 *Phys. Rev.* **83** 34
[8] Landau L D and Lifshitz E M 1980 *Statistical Physics. Part 1: Course of Theoretical Physics* vol 5 (Oxford: Pergamon)
[9] Majorana E 1937 *Nuovo Cimento* **14** 171
[10] Fu L and Kane C L 2008 *Phys. Rev. Lett.* **100** 096407

[11] Fu L and Kane C L 2009 *Phys. Rev.* B **79** 161408(R)
[12] Lutchyn R M, Sau J D and Das Sarma S 2010 *Phys. Rev. Lett.* **105** 077001
[13] Oreg Y, Refael G and von Oppen F 2010 *Phys. Rev. Lett.* **105** 177002
[14] Yu Kitaev A 2001 *Phys.–Usp* **44** 131
[15] Alicea J 2012 *Rep. Prog. Phys.* **75** 076501
[16] Flensberg K 2012 *Semicond. Sci. Technol.* **27** 124003
[17] Sato M and Fujimoto S 2016 *J. Phys. Soc. Japan* **85** 072001
[18] Albrecht S M, Higginbotham A P, Madsen M, Kuemmeth F, Jespersen T S, Nygård J, Krogstrup P and Marcus C M 2016 *Nature* **531** 206
[19] Mourik V, Zuo K, Frolov S M, Plissard S R, Bakkers E P A M and Kouwenhoven L P 2012 *Science* **336** 1003
[20] Hewson A C 1997 *The Kondo Problem to Heavy Fermions* (Cambridge: Cambridge University Press)
[21] Fidkowski L, Alicea J, Lindner N H, Lutchyn R M and Fisher M P A 2012 *Phys. Rev.* B **85** 245121
[22] Kundu A and Seradjeh B 2013 *Phys. Rev. Lett.* **111** 136402
[23] Ilan R, Bardarson J H, Sim H S and Moore J E 2014 *New J. Phys.* **16** 053007
[24] Lobos A M and Das Sarma S 2015 *New J. Phys.* **17** 065010
[25] Wang R, Lu H Y, Wang B and Ting C S 2016 *Phys. Rev.* B **94** 125146
[26] Lutchyn R M and Glazman L I 2017 arXiv:1701.00184
[27] Smirnov S 2015 *Phys. Rev.* B **92** 195312
[28] Liu D E, Cheng M and Lutchyn R M 2015 *Phys. Rev.* B **91** 081405(R)
[29] Liu D E, Levchenko A and Lutchyn R M 2015 *Phys. Rev.* B **92** 205422
[30] Beenakker C W J 2015 *Rev. Mod. Phys.* **87** 1037
[31] Valentini S, Governale M, Fazio R and Taddei F 2016 *Physica* E **75** 15–21
[32] Sela E, Oreg Y, von Oppen F and Koch J 2006 *Phys. Rev. Lett.* **97** 086601
[33] Ferrier M, Arakawa T, Hata T, Fujiwara R, Delagrange R, Weil R, Deblock R, Sakano R, Oguri A and Kobayashi K 2016 *Nat. Phys.* **12** 230
[34] Smirnov S and Grifoni M 2013 *New J. Phys.* **15** 073047
[35] Smirnov S and Grifoni M 2013 *Phys. Rev.* B **87** 121302(R)
[36] Altland A and Simons B 2010 *Condensed Matter Field Theory* 2nd edn (Cambridge: Cambridge University Press)
[37] Wang E *et al* 2013 *Nat. Phys.* **9** 621
[38] Vernek E, Penteado P H, Seridonio A C and Egues J C 2014 *Phys. Rev.* B **89** 165314
[39] Goldhaber-Gordon D, Shtrikman H, Mahalu D, Abusch-Magder D, Meirav U and Kastner M A 1998 *Nature* **391** 156
[40] Haim A, Berg E, von Oppen F and Oreg Y 2015 *Phys. Rev.* B **92** 245112